Growth of 2D GaN Single Crystals on Liquid Metals

Yunxu Chen,[§,†] Keli Liu,[§,‡] Jinxin Liu,[†] Tianrui Lv,[†] Bin Wei,[#] Tao Zhang,[†] Mengqi Zeng[†], Zhongchang Wang[#] and Lei Fu*[,†]

[†]College of Chemistry and Molecular Sciences, Wuhan University, Wuhan 430072, P. R. China
[‡]The Institute for Advanced Studies (IAS), Wuhan University, Wuhan 430072, China
[#]Department of Quantum and Energy Materials, International Iberian Nanotechnology Laboratory (INL), 4715-330 Braga, Portugal

[§]*These authors contributed equally to this work.*

[*]*To whom correspondence should be addressed: email: leifu@whu.edu.cn*

1. Experiments and characterizations

Pretreatment: Divide a commercial gallium (Ga) pellet (Alfa Aesar, 99.9999% purity) into small droplets in hot ethanol and then frozen into tiny Ga balls. The tungsten (W) foils (W foils with a purity of 99.95 wt. % were purchased from Alfa Aesar China (Tianjin) Co. Ltd. and Shanghai Minor Metals Co. Ltd.). The W foils were ultra-solicited and rinsed with acetone, ethanol and deionized water prior to being dried under air stream. A Ga ball (about 1 mg) was placed on a W foil (0.5×0.5 cm^2).The urea (Shanghai Hush Laboratorial Equipment, analytical purity) in a quartz boat was heated to 160 ºC in a quartz tube furnace (HTF 55322C Lindberg/Blue M) under ambient pressure and then exposed for 5 min under 100~200 sccm Ar, 10~30 sccm H_2.

Chemical vapor deposition (CVD) process: The growth process is consisted of five steps: (1) placing the pretreated urea (≈10 mg) as the precursor in the upstream of the furnace, zone 1; (2) placing the Ga–W substrates in the position away from the center region of the quartz tube furnace, zone 2; (3) heating the Ga–W substrates to 1080 ºC at a rate of 30 ºC/min under the flow of Ar and H_2; (4) removing the quartz tube until Ga–W substrates are in the center region of the quartz tube furnace; (5) exposing the substrates for 5~10 min under 200~300 sccm Ar, and 10~30 sccm H_2; (6) cooling the substrates to the room temperature rapidly under the flow of Ar and H_2.

Transferring the two dimensional (2D) gallium nitride (GaN) crystals to the target substrates: The process of transferring the samples to the target substrates involves spin-coating a poly (methyl methacrylate) (PMMA) film onto the substrate with GaN single crystals grown on it and releasing the PMMA/sample film by etching out Ga with diluted hydrogen chloride (1:4) for 10~12 h. This was followed by a rinsing in ultra-pure water to remove the metal ions. The PMMA layer was dissolved with hot acetone after the PMMA/sample film was transferred onto the target substrates, such as 300 nm SiO_2/Si substrates and the copper TEM grid.

Device fabrication: Firstly, this GaN single crystal with 25 μm in lateral size was transferred on SiO_2/Si substrate with 300-nm-thick oxide layer. Secondly, two exfoliated few-layered graphene flakes were transferred onto the surface of 2D GaN single crystal assisted by PMMA. Then, the source and drain electrodes of obtained sample were defined by electron beam lithography (EBL) in a scanning electron microscope (SEM), followed by thermal evaporation of Cr/Au (15/50 nm) electrode layer. Finally, the sample was immersed with acetone followed by isopropyl alcohol cleaning, leading to the formation of patterned electrodes.

Electrical measurements: Field effect transistor (FET) devices were fabricated to probe the intrinsic electrical properties of the 2D GaN single crystals with a thickness of 4.8 nm, in which the channel length is ~19.4 μm and the channel width is ~9.3 μm. All the FET measurements were executed at room temperature in the air. The current (I)−voltage (V) characteristic curves were collected in a probe station under ambient conditions using an Agilent 4155C.

Characterization: Raman spectroscopy was performed with a laser micro-Raman spectrometer (Renishaw in Via, 532 nm excitation wavelength). The photoluminescence (PL) spectra with the excitation wavelength of 325 nm and 266 nm were carried out using LabRAM HR, Horiba JobinYvon (the utilized excitation power was 3 mW). Both the Raman spectra and PL spectra were extracted from the samples transferred onto the Si/SiO_2 substrates. The X-ray photoelectron spectroscopy (XPS) measurements were conducted using a Thermo Scientific, ESCALAB 250Xi. The measuring spot size was 500 μm and the binding energies were calibrated by referencing the C 1s peak (284.8 eV). The XPS depth profiling was performed by Ar ionic bombardment to gradually remove the surface layers. Etching was conducted for 8 times, and each etching took about 100 seconds. The XPS spectra for confirming the chemical composition of GaN crystals were collected from the samples that were transferred onto the Si/SiO_2 substrates. While the XPS depth profiling spectra were directly extracted from Ga–W substrates after the growth of GaN to investigate the growth process. The atomic force microscope (AFM) images were taken with an environmental atomic force microscope (Cypher ES, Asylum Research) with samples transferred onto the 300 nm SiO_2/Si. The transmission electron microscopy (TEM) images were obtained by an aberration-corrected high-resolution TEM (HRTEM) system (FEI Titan 80−300) with an operating voltage of 80 kV and by a probe-corrected high-resolution TEM system (Titan Probe corrected TEM, Titan G2 60−300) with an operating voltage of 300 kV. The scanning TEM (STEM) images were obtained using a probe Cs-corrected TEM (FEI Titan ChemiSTEM) with the high-angle annular dark-field (HAADF) and the bright-field (BF) imaging techniques. And the energy dispersive X-ray spectroscopic (EDS) measurements were used to collect the elemental mapping of the as-prepared samples. The FEI Titan abberation-corrected ChemiSTEM was operated at 200 kV with a spot size of 7# and 8#, camera length of 135 mm, condenser aperture of 70 and 100 μm, and convergent angle 21 and 30 mrad. The samples were transferred onto a quantifoil copper TEM grid for structural characterization.

2. Sketch map of the growth process

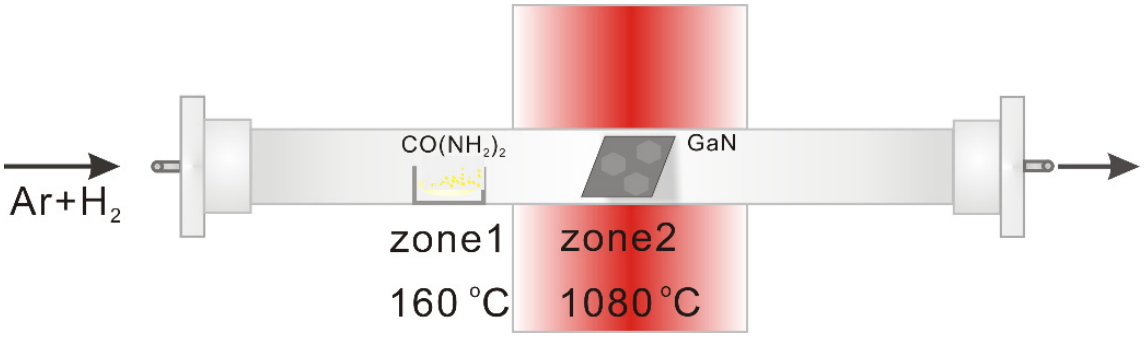

Figure S1. Sketch map of the CVD procedure for 2D GaN single crystals at the ambient pressure.

The urea ($CO(NH_2)_2$) powders were put a few centimeters away from the zone 1, while the Ga pellet that was supported by the W foil was placed in zone 2. Firstly, the molten Ga could spread out on the W surface when the temperature of the zone 2 was up to 1080 ºC. Secondly, the urea precursors were moved into the zone 1, which had already been heated to 160 ºC. With urea ($CO(NH_2)_2$) powders as precursors, the 2D GaN can then be formed on the liquid gallium surfaces at 1080 ºC via a surface-confined nitridation reaction (SCNR).

3. The statistical analyses of the lateral size and thickness of the 2D GaN single crystals

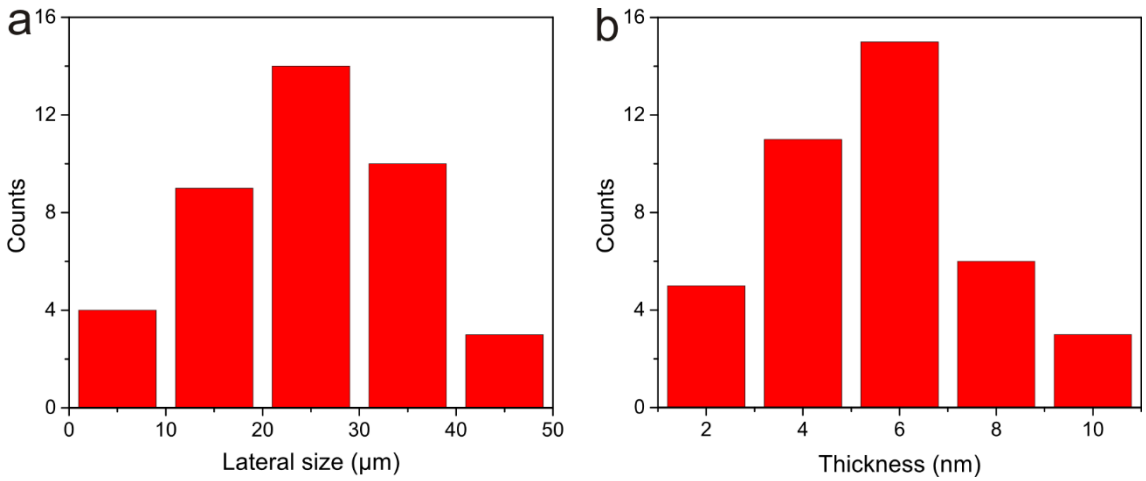

Figure S2. (a, b) Statistical distributions of the lateral size and thickness of 2D GaN single crystals.

The lateral size and thickness distributions of 2D GaN single crystals obtained via the SCNR strategy are analyzed. The statistical results shown in Figure S2a indicated the distribution of the grain sizes, where the average value of them was calculated to be ~26 μm. Moreover, the thickness distribution with an average value of ~5.6 nm was also revealed by the statistical result in Figure S2b.

4. XPS spectra for confirming the chemical composition of the 2D GaN single crystals

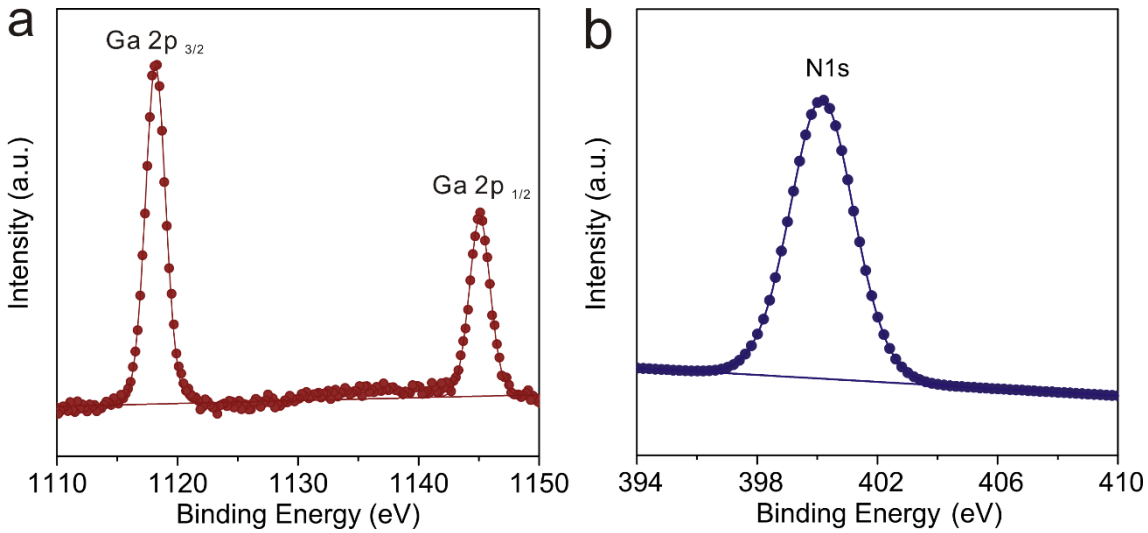

Figure S3. (a, b) XPS spectra for the Ga 2p peaks and N 1s peaks for the as-grown 2D GaN single crystals, respectively.

XPS spectra (Figure S3a–b) were collected to confirm the chemical composition of the GaN crystals that were transferred onto 300 nm SiO_2/Si. The primary spin-orbital components $2p_{1/2}$ and $2p_{3/2}$ of Ga 2p are located at 1143.8 and 1116.7 eV, respectively. The N1s components show a dominant peak at the binding energy of 399.5 eV. All these peaks are in accordance with the previous reports.[1] No characteristic peaks attributed to gallium oxide or oxynitride were detected, demonstrating the high purity of the 2D GaN single crystals.

5. The atomic structure of the 2D GaN crystals along the [0001] zone axis

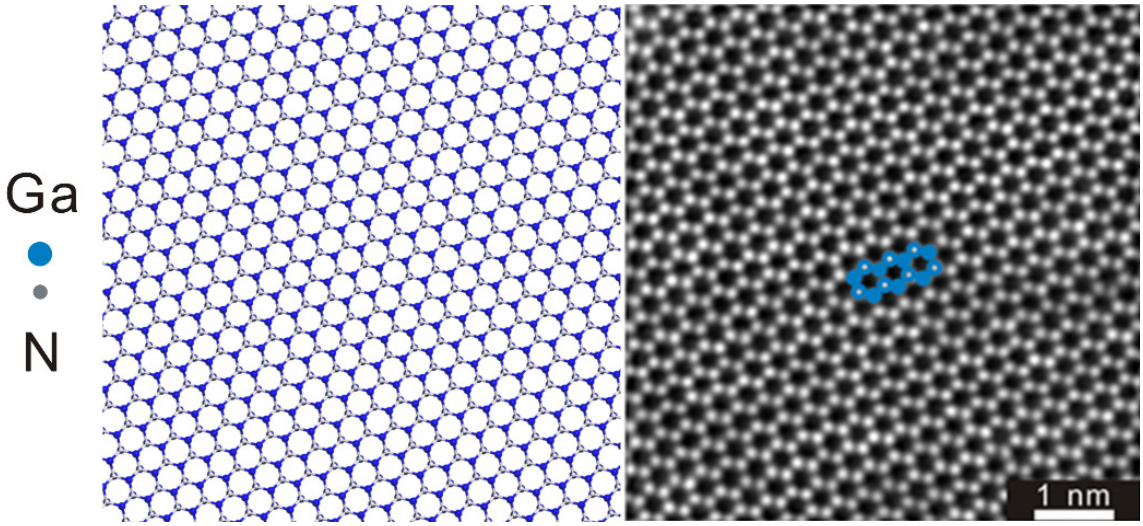

Figure S4. Atomic model and HAADF STEM imaging simulation of the 2D GaN crystal acquired along [0001] zone axis.

6. HRTEM images for confirming the crystal plane distance of 2D GaN single crystals

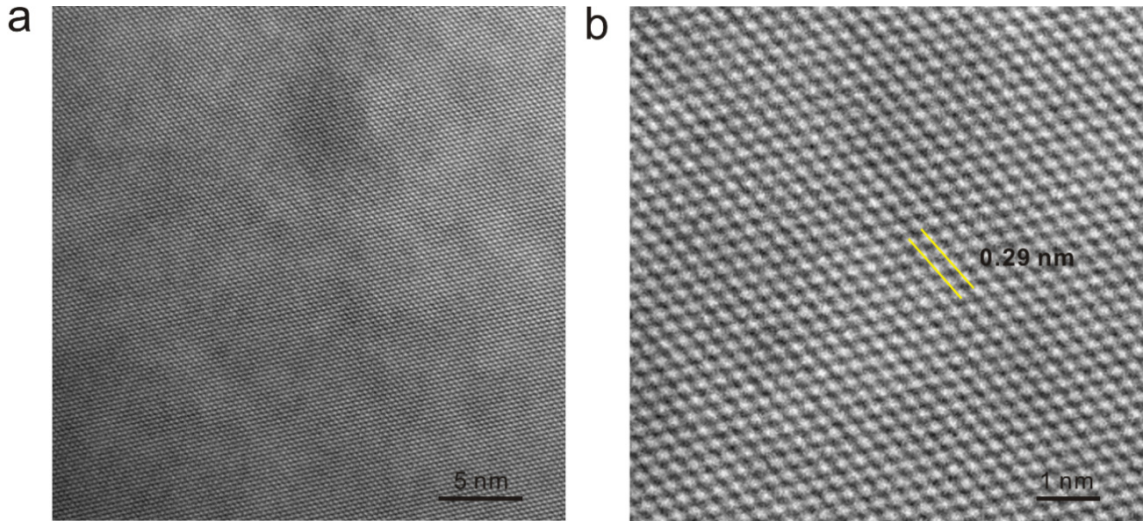

Figure S5. TEM for confirming the crystal plane distance of 2D GaN single crystals. (a) HRTEM atomic image. (b) Magnified HRTEM atomic image.

7. SAED patterns for confirming the uniformly incremental lattice

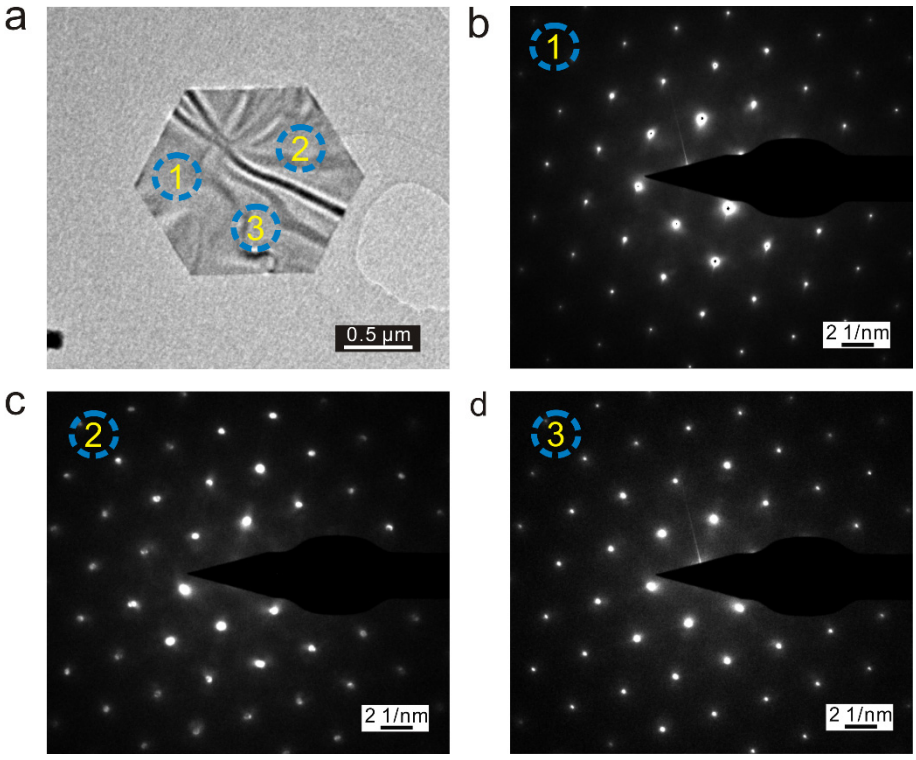

Figure S6. Confirmation of the uniform incremental lattice of the 2D GaN single crytal. (a) A low magnification TEM image of a hexagonal single crystal. (b−d) SAED patterns collected from crystal in (a) at three different regions, as indicated by the three bule dased circles shown in (a).

8. Fast Fourier transform (FFT) of the 2D GaN crystals in [10$\bar{1}$0] zone axis

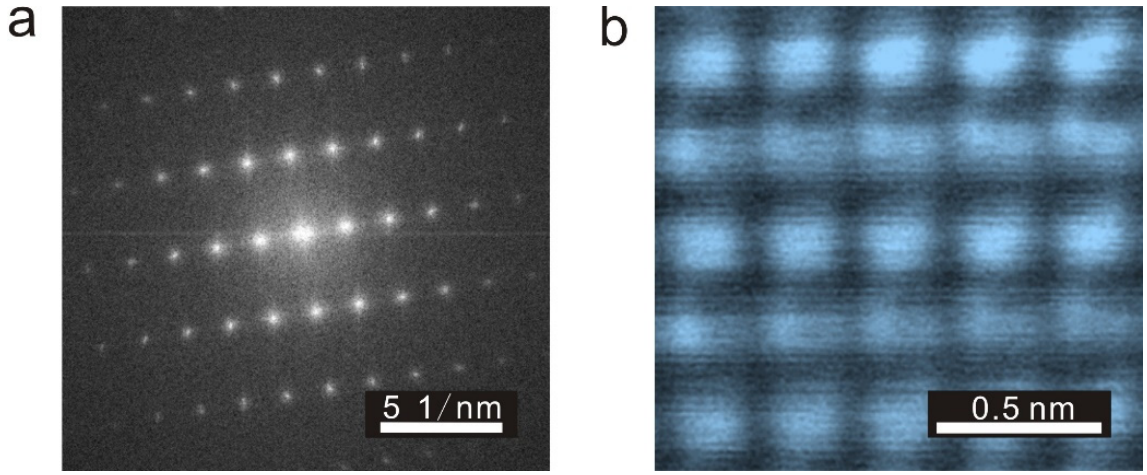

Figure S7. (a) FFT of the 2D GaN crystals in [10$\bar{1}$0] zone axis collected from the image in (b). (b) High-resolution aberration-corrected HAADF STEM image viewed on (10$\bar{1}$0) plane.

9. Thickness-dependent PL characterizations

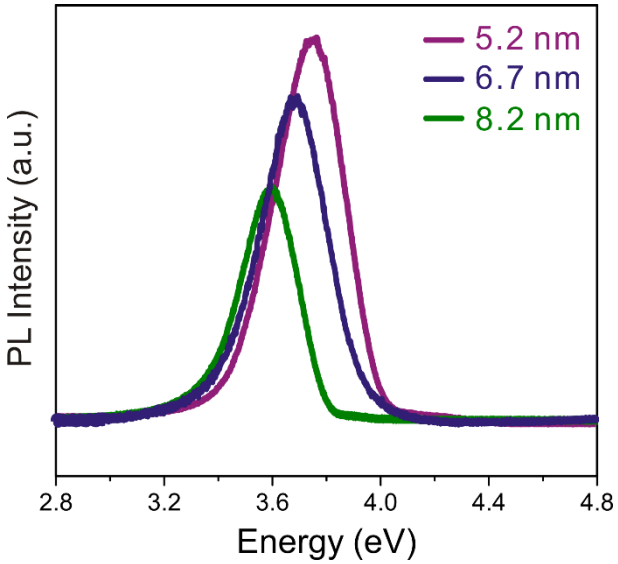

Figure S8. Thickness-dependent PL spectra of the 2D GaN single crystals.

As shown in Figure S8, PL spectra of 2D GaN crystals with different thickness have been collected to elucidate the thickness-dependent characteristics. The 2D crystals with the thickness of 5.2 nm, 6.7 nm and 8.2 nm exhibited the obviously different photon energy of 3.76 eV, 3.68 eV and 3.60 eV, indicating that the photon energy increases with the decrease of crystals thickness. This thickness-dependent photon energy variation behavior of GaN is consistent with the previous reports.[2,3] Additionally, the increased PL intensity with the decrease in thickness reveals the higher internal quantum efficiency and stronger excitonic effects of 2D GaN crystals, which are caused by quantum confinement effect.[4,5] The GaN crystals with thinner thickness may be more suitable for UV-emission devices due to the deeper UV photon energy and stronger excitonic effects.

10. Temperature-dependent PL characterizations

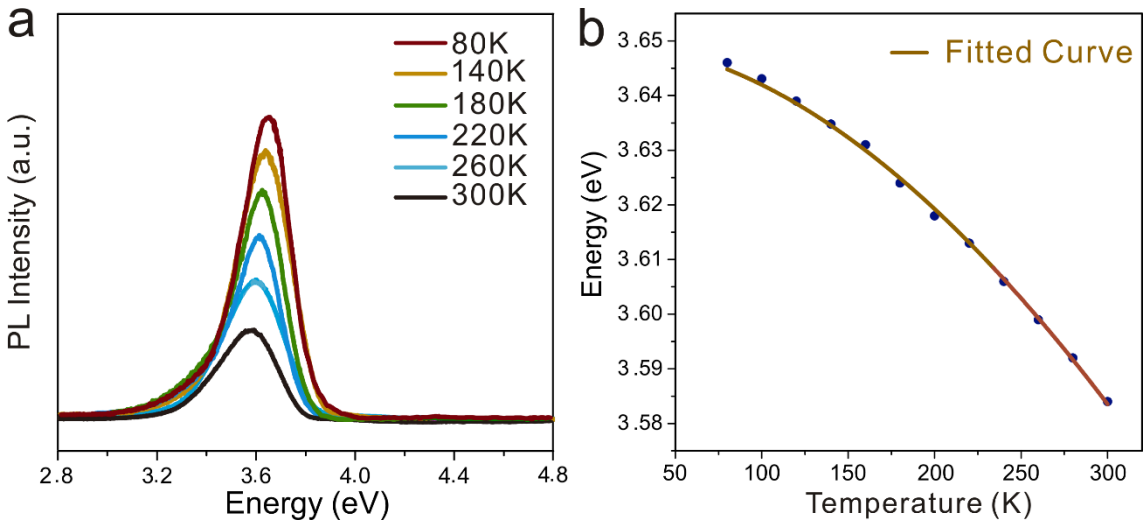

Figure S9. (a) Temperature-dependent PL spectra from a 2D GaN single crystal with a thickness of 8.7 nm. (b) Peak energy for the 2D GaN emission from Figure S9a fitted as a function of the measurement temperature. The brown solid line is the fitted curve based on the Varshni equation. The Varshni parameters utilized here for the fitted curve are $\alpha = (8.5 \pm 0.6) \times 10^{-1}$ eV^{-1} K^{-1} and $\beta = 830 \pm 21$ K.

Temperature dependent PL measurements were performed on a GaN single crystal with a thickness of 8.7 nm to further reveal their characteristics (Figure S9a). The PL spectrum exhibits a dominant band gap of 3.58 eV at 300 K, and it gradually shifts to the higher-energy region with the decrease of the temperature. The variation of band gap peak position with temperature is plotted in Figure S9b, and the variation tendency is analyzed based on the Varshni equation.[6] S-type (decrease-increase-decrease) behavior cannot be observed, indicative of the absence of any compositional inhomogeneity or clusters in the 2D GaN single crystal.[7,8]

11. Schematic of the SCNR strategy for growing 2D GaN

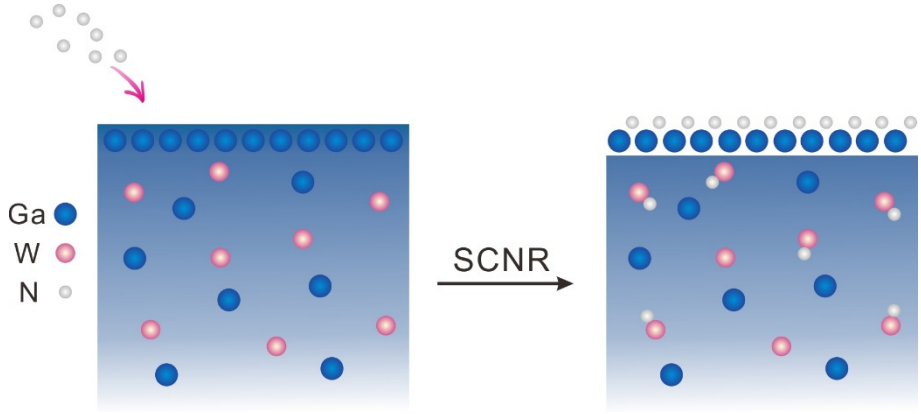

Figure S10. Schematic of the SCNR strategy for the growth of 2D GaN single crystals.

Firstly, the Ga–W substrates (the W foil with a Ga pellet of 1 mg on its surface) were heated to 1080 ºC in the H_2 atmosphere. The surface tension of molten W metal (2361.5 $mN \cdot m^{-1}$) is far larger than that of Ga (628.7 $mN \cdot m^{-1}$).[9] Hence, the outmost surface area is occupied by the Ga atoms with weak interactions, further inducing the formation of Ga/Ga–W structure (where the surface is ultrathin Ga layer, while the subsurface is Ga–W solid solution). Based on the designed Ga/Ga–W structure, the SCNR will occur during CVD procedure, as illustrated in Figure S10. Thereinto, with the surficial atomic Ga layer serving as templates and urea as nitrogen source, micron-sized 2D GaN can be obtained. Meanwhile, the sub-surficial Ga–W solid solution can impede the thickening of 2D GaN owing to the stronger nitridation ability of W atoms than that of Ga atoms. Thus, the confined growth behavior for 2D GaN on the surface of the molten system could be realized.

12. XPS depth profiles for identifying the Ga/Ga–W structure

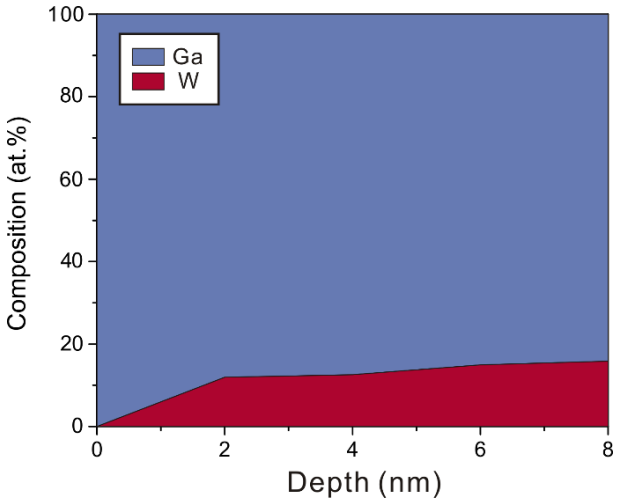

Figure S11. XPS depth profile to identify the Ga and W distributions in the molten Ga/Ga–W structure.

For the molten Ga/Ga–W structure, the outmost surface is consisted of Ga. While at the subsurface (at the depth of 2 nm) of the molten Ga/Ga–W structure, the composition proportion of W atoms increases obviously. Thus, the Ga/Ga–W structure with an ultrathin Ga layer at its outmost surface can be confirmed.

13. XPS deep analysis for confirming the SCNR process

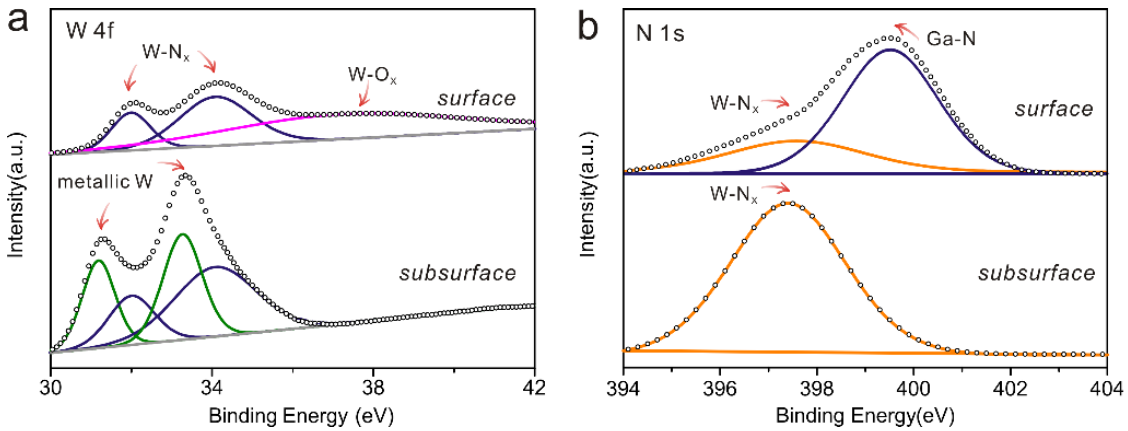

Figure S12. (a, b) XPS depth analysis of Ga–W substrates after GaN growth for W 4f (a), N 1s (b) respectively.

XPS deep analysis was conducted on the molten Ga/Ga−W system after nitridation, as shown in Figure S12. The double peaks located at 34.0 eV and 32.5 eV were consistent with the W $4f_{5/2}$ and W $4f_{7/2}$ of WN_x species, respectively.[10] For N 1s presented in Figure S12b, the peaks located at 397.6 eV are associated with the WN_x species.[10] GaN can be detected only on the outmost surface, while the WN_x species can only be detected inside (Figure S12b). Here, the WN_x species can be probed on the surface due to inevitable thermodynamic diffusion of W atoms at elevated temperature.[11] Metallic W constituents can be detected in the bulk of molten Ga/Ga−W system after nitridation (Figure S12a), demonstrating the adequate W atoms in the sub-surficial Ga−W solid solution.

In the inner Ga−W solid solution, it is easier for the formation of W−N bonds than Ga−N bonds due to the lower Gibbs free energy of WN (–121 kJ mol^{-1}) than that of GaN (–18 kJ mol^{-1}), thus the formation of GaN can be effectively suppressed in the subsurface of molten Ga/Ga−W system, leading to the formation of ultrathin GaN single crystals.

Reference

(1) Thakur, V.; Shivaprasad, S. M. Electronic structure of GaN nanowall network analysed by XPS. *Appl. Surf. Sci.* **2015**, *327*, 389.

(2) Ramakrishna Matte, H. S. S.; Gomathi, A.; Manna, A. K.; Late, D. J.; Datta, R.; Pati, S. K.; Rao, C. N. R. MoS_2 and WS_2 analogues of graphene. *Angew. Chem. Int. Ed.* **2010**, *49*, 4059.

(3) Zhao, Y.; Qiao, J.; Yu, P.; Hu, Z.; Lin, Z.; Lau, S. P.; Liu, Z.; Ji, W.; Chai, Y. Extraordinarily strong interlayer interaction in 2D layered PtS_2. *Adv. Mater.* **2016**, *28*, 2399.

(4) Islam, S. M.; Protasenko, V.; Lee, K.; Rouvimov, S.; Verma, J.; Xing, H.; Jena, D. Deep-UV emission at 219 nm from ultrathin MBE GaN/AlN quantum heterostructures. *Appl. Phys. Lett.* **2017**, *111*, 091104.

(5) Sanders, N.; Bayerl, D.; Shi, G.; Mengle, K. A.; Kioupakis. E. Electronic and optical properties of two-dimensional GaN from first-principles. *Nano Lett.* **2017**, *17*, 7345.

(6) Varshni, Y. P. Temperature dependence of the energy gap in semiconductors. *Physica* **1967**, *34*, 149.

(7) Nepal, N.; Li, J.; Nakarmi, M. L.; Lin, J. Y.; Jiang, H. X. Exciton localization in AlGaN alloys. *Appl. Phys. Lett.* **2006**, *88*, 062103.

(8) Steude, G.; Meyer, B. K.; Göldner, A.; Hoffmann, A.; Bertram, F.; Christen, J.; Amano, H.; Akasaki, I. Optical investigations of AlGaN on GaN epitaxial films. *Appl. Phys. Lett.* **1999**, *74*, 2456.

(9) Mills, K. C.; Su, Y. C. Review of surface tension data for metallic elements and alloys: Part 1- Pure metals. *Inter. Mater. Rev.* **2013**, *51*, 329.

(10) Wen, M.; Meng, Q. N.; Yu, W. X.; Zheng, W. T.; Mao, S. X.; Hua, M. J. Growth, stress and hardness of reactively sputtered tungsten nitride thin films. *Surf. Coat. Technol.* **2010**, *205*, 1953

(11) Zeng, M.; Chen, Y.; Li, J.; Xue H.; Mendes, R. G.; Liu, J.; Zhang, T.; Rümmeli, M. H.; Fu, L. 2D WC single crystal embedded in graphene for enhancing hydrogen evolution reaction. *Nano Energy* **2018**, *33*, 356.